Frequency stability improvement for piezoresistive micromechanical oscillators via synchronization

Cite as: AIP Advances **7**, 035204 (2017); https://doi.org/10.1063/1.4978222
Submitted: 17 January 2017 • Accepted: 23 February 2017 • Published Online: 07 March 2017

Dong Pu, Ronghua Huan and Xueyong Wei

Frequency stability improvement for piezoresistive micromechanical oscillators via synchronization

Dong Pu,[1] Ronghua Huan,[1,a] and Xueyong Wei[2,b]
[1]*Department of Mechanics, Key Laboratory of Soft Machines and Smart Devices of Zhejiang Province, Zhejiang University, Hangzhou 310027, China*
[2]*State Key Laboratory for Manufacturing Systems Engineering, Xi'an Jiaotong University, Xi'an 710049, China*

(Received 17 January 2017; accepted 23 February 2017; published online 7 March 2017)

Synchronization phenomenon first discovered in Huygens' clock shows that the rhythms of oscillating objects can be adjusted via an interaction. Here we show that the frequency stability of a piezoresistive micromechanical oscillator can be enhanced via synchronization. The micromechanical clamped-clamped beam oscillator is built up using the electrostatic driving and piezoresistive sensing technique and the synchronization phenomenon is observed after coupling it to an external oscillator. An enhancement of frequency stability is obtained in the synchronization state. The influences of the synchronizing perturbation intensity and frequency detuning applied on the oscillator are studied experimentally. A theoretical analysis of phase noise leads to an analytical formula for predicting Allan deviation of the frequency output of the piezoresistive oscillator, which successfully explains the experimental observations and the mechanism of frequency stability enhancement via synchronization. [http://dx.doi.org/10.1063/1.4978222]

Micro and nano mechanical resonators have been widely studied as a potential alternative to conventional quartz oscillators due to their advantages such as easier to miniaturize and to be integrated with electronics.[1,2] As frequency control or time reference devices, micromechanical oscillators have to own a better frequency stability. However, their performances are often degraded by large displacement instabilities due to scaling effect and nonlinearity,[3–5] frequency noise imposed by thermomechanical noise[6–8] and intrinsic frequency fluctuations.[9] According to the comprehensive literature review by Sansa et al.,[9] there still has several orders of magnitude over the thermo-mechanical noise limit to improve the frequency stability for micro/nanomechanical oscillators.

Synchronization phenomenon first discovered in Huygens' clock shows that the rhythms of oscillating objects can be adjusted via an interaction[10] and accordingly synchronization is considered to be an effective technique to overcome the frequency dispersing. In recent few years, special efforts have been invested in the reduction of phase noise and the improvement frequency stability in micro/nanomechanical oscillators via synchronization. An improvement of the frequency stability is observed when two micromechanical oscillators are synchronized.[11] The phase noise can be significantly reduced when two anharmonic nanomechanical oscillator in the phase synchronized state.[12] In the previous work,[13] one micromechanical oscillator is synchronized to an external force and the phase noise spectrum is given analytically which implies that the largest phase noise reduction occurs in the center of the Shapiro step. Different from the oscillators reported in those studies, piezoresistive micromechanical oscillators are proposed recently because of their better electrical transduction efficiency but the induced joule heating is believed to affect their stability of frequency output. In

[a]Electronic mail: rhhuan@zju.edu.cn
[b]Electronic mail: seanwei@mail.xjtu.edu.cn

this work, the synchronization phenomenon in a piezoresistive micromechanical clamped-clamped (C-C) beam oscillator is investigated and the observed improvement of frequency stability is studied.

The piezoresistive oscillator is built up on a micromechanical C-C beam resonator that is fabricated by a standard Silicon-On-Insulator (SOI) process. Fig. 1 shows a microscopic picture of the micro-resonator and a schematic drawing of the oscillator circuit.[4] The dimensions of the resonator are $478\mu m$ long, $10\mu m$ wide and $10\mu m$ thick respectively. It is electrostatically actuated in its principle flexural mode. The high impedance of resonators at resonance makes other transduction methods (such as piezoresistive and piezoelectric) popular except using the capacitive transduction to detect the mechanical resonance. Here, the differential piezoresistive sensing method is used to detect the transverse displacement.[14] After amplification, the resulting signal is filtered and phase shifted by a prescribed amount of ϕ_0. Then the square wave signal with a fixed amplitude V_{ac2} from the comparator is applied on the comb-drive electrode to electrostatically drive the resonator. The feedback time-varying driving force compensates the energy dissipation and in the absence of any external perturbations, this closed loop feedback sustains the beams vibration at an amplitude A_0 and a frequency Ω_0. To entrain the oscillator into synchronized motion, an external harmonic signal of amplitude V_{ac1} and frequency Ω_s is applied on the other comb-drive electrode as a perturbation force to the beam oscillator. A frequency counter (Agilient 53230A) is used to log the frequency output of the piezoresistive oscillator.

The equation of motion for the forced self-sustained nonlinear micromechanical beam's oscillation is well described using the Duffing equation.

$$m\ddot{x} + \mu\dot{x} + k_1 x + k_3 x^3 = F_{act} \tag{1}$$

Where, m, μ, k_1, k_3 and F_{act} are the effective mass, damping coefficient, linear mechanical stiffness, cubic mechanical stiffness and the actuation force, respectively. The micro-beam is actuated electrostatically and the driving force F_{act} combining the self-sustaining force with the synchronization perturbation can be expressed as follow.

$$\begin{aligned} F_{act} = & \frac{1}{2}\left|\frac{\partial C_2}{\partial x}\right|(V_{dc2} + V_{ac2}\mathrm{sgn}(\cos\phi_t))^2 \\ & - \frac{1}{2}\left|\frac{\partial C_1}{\partial x}\right|(V_{dc1} + V_{ac1}\cos\Omega_s t)^2 \end{aligned} \tag{2}$$

Where, $\frac{\partial C_1}{\partial x}$ and $\frac{\partial C_2}{\partial x}$ are capacitance gradients,V_{dc1} and V_{dc2} are DC driving voltages, $\phi_t = \phi + \phi_0$ is the instantaneous oscillation phase of the coordinate $x(t)$. In our experiment, the AC driving voltage

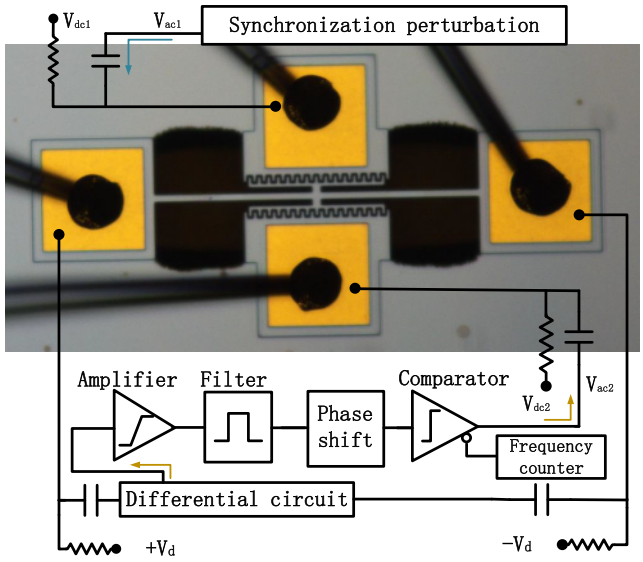

FIG. 1. An optical graph of micro beam resonator and the schematic drawing of the closed-loop circuit used in this work.

is much smaller than DC voltage. The capacitance gradient can be expanded in Taylor's series and accordingly the driving force can be simplified as follow.

$$F_{act} = F_0 \mathrm{sgn}(\cos\phi_t) + F_s \cos\Omega_s t + k_{1e}x + k_{3e}x^3 \tag{3}$$

Where k_{1e},k_{3e},F_0,F_s are respectively the linear electric spring constant, nonlinear electric spring constant, the self-sustaining force and the external perturbation. The main resonance region is discussed here and the parametric terms are neglected. Redefining time units and normalizing the Eq. 1 by the spring constant $k(k = k_1 - k_{1e})$ leads to the following equation of the oscillation.

$$\ddot{x} + Q^{-1}\dot{x} + x + \beta x^3 = f_0 \mathrm{sgn}(\cos\phi_t) + f_s \cos\Omega_s' \tau \tag{4}$$

Where, $Q = \frac{\sqrt{km}}{\gamma}$, $\beta = \frac{k_3 - k_{3e}}{k}$, $f_0 = \frac{F_0}{k}$, $f_s = \frac{F_s}{k}$, $\Omega_s' = \Omega_s\sqrt{\frac{m}{k}}$, $\tau = \sqrt{\frac{k}{m}}t$. Here Q is the quality factor, the cubic-term coefficient β is positive (negative) depending on the hardening (k_3) and softening (k_{3e}) nonlinearities. The self-sustaining force f_0 reaches the maximal when ϕ_0 is $\pi/2$. The sign function is expanded and simplified as follow after neglecting the higher order harmonics.

$$\mathrm{sgn}(\cos\phi_t) \approx -\frac{4}{\pi}\sin(\phi) \tag{5}$$

For the self-excited oscillation without external perturbation ($f_s = 0$), the frequency Ω_0 and amplitude A_0 can be expressed as follows by using the method applied by Antonio.[5]

$$\Omega_0 = \frac{1}{\sqrt{2}}\left(1 + \left(1 + \frac{48\beta Q^2 f_0^2}{\pi^2}\right)^{\frac{1}{2}}\right)^{\frac{1}{2}}, A_0 = \frac{4Qf_0}{\pi\Omega_0} \tag{6}$$

When a harmonic perturbation is applied ($f_s \neq 0$), there exists a synchronization region [$\Omega_0 - \frac{1}{2}\Omega_c, \Omega_0 + \frac{1}{2}\Omega_c$] within which the frequency of mechanical oscillator Ω_0' locks to synchronizing frequency Ω_s and the synchronization bandwidth Ω_c is derived as follow.

$$\Omega_c = \frac{\pi f_s}{4f_0 Q}\left(\left(\frac{24\beta Q A_0^2}{\pi\Omega_0}\right)^2 + 1\right)^{\frac{1}{2}} \tag{7}$$

This synchronization region of the oscillator synchronized to an external force can also be obtained similarly using averaging method.[13] Fig. 2 shows the synchronization region at various perturbation intensities (V_{ac1}) predicted using Eq. 7. It is clear that the synchronization bandwidth is 170.5Hz at V_{ac1} of 20mV and increases as the harmonic perturbation intensity increases. In the verifying experiments, the beam micro-resonator is tested in a vacuum chamber with the air pressure

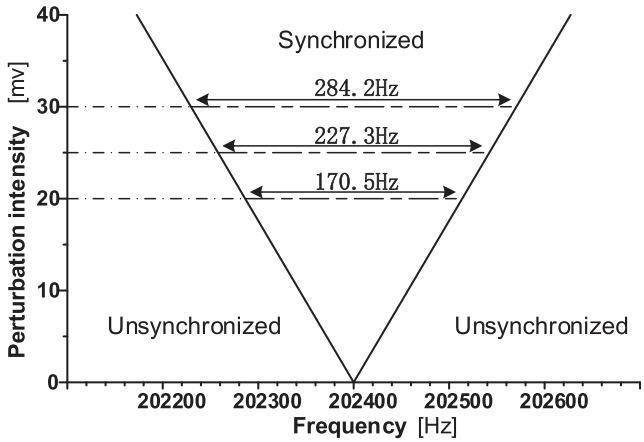

FIG. 2. The effect of perturbation intensity (V_{ac1}) on the synchronization bandwidth (Ω_c). The parameters used for prediction are all obtained from measurements that $Q \approx 11734$, $\beta = 3.45 \times 10^9$ respectively.

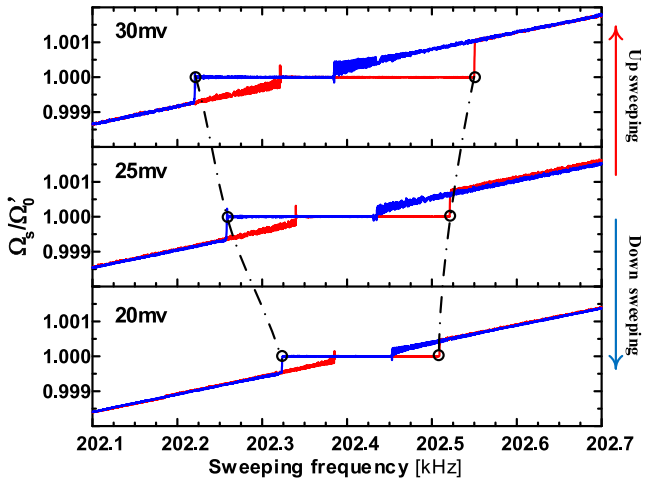

FIG. 3. The frequency ratio Ω_s/Ω_0' measured by sweeping Ω_s at different perturbation intensities.

less than 0.01Pa. The resonator is driven into oscillation and a harmonic signal from a RF source (Agilient 33250A) is applied to perturb the oscillation. The free-running self-oscillation frequency is 202400Hz. Both the frequency outputs from the signal generator and the piezoresistive oscillator are logged simultaneously using the dual channel frequency counter. The frequency ratio Ω_s/Ω_0' is obtained and plotted against Ω_s as shown in Fig. 3.

It is obvious that there is a synchronization region in which the frequency of external perturbation equals that of the piezoresistive oscillator. The synchronization bandwidths are respectively 185.7Hz, 262.1Hz and 328.8Hz for V_{ac1} of 20mV, 25mV and 30mV, which are close to the analytical predictions shown in Fig. 2 and confirm that the synchronization bandwidth can be tuned by the intensity of harmonic perturbation (or the signal to perturbation ratio SPR=$f_s/f_0 \propto V_{ac1}/V_{ac2}$). By sweeping up and down using different perturbation intensities, the Arnold tongue is figured out by connecting the edges with dashed lines.

In the synchronization region, a series of experiments on frequency stability are performed at various frequency detunings $\delta\Omega$ ($\delta\Omega = \Omega_s - \Omega_0$) and a fixed perturbation intensity (V_{ac1}=10mV). Allan deviations of frequency outputs from the piezoresistive oscillator are plotted in Fig. 4 comparing with that of the free running oscillator and the synchronizing RF source. It clearly shows that the frequency stability of the piezoresistive oscillator is enhanced as compared with that of the oscillator before synchronization, but there is no much difference in the frequency stability for different frequency detunings in the synchronization region, which indicates that the intensity of harmonic perturbation has greater effect on the frequency stability than the frequency of perturbation.

To further confirm this, a series of experiments on frequency stability are performed at various intensities of harmonic perturbation V_{ac1} from 10mV to 50mV, a fixed self-sustaining amplitude V_{ac2}=400mV and a fixed frequency of harmonic perturbation located in the center of synchronization region. Allan deviation of the oscillator frequency output is calculated as a function of integration time τ_A from 100ms to 100s as shown in Fig. 5. It is clearly shown that the frequency stability can be improved nearly 10 folds at τ_A=2s. For a linearly increasing SPR, we can find the frequency stability can be enhanced gradually with slow growth. Intuitively, a bigger SPR brings a better synchronization state which leads to better frequency stability. Interestingly, the frequency stability is not linearly improved.

In order to better understand these phenomena of improving frequency stability via synchronization, a theoretical investigation is conducted. A model of micromechanical oscillator synchronized to an external force in a noisy environment has been put forward by Shoshani[13] and the phase noise spectrum is given. Starting from this point, a normalized equation of our closed loop oscillator affected by additive noise ξ_1, multiplicative noise ξ_2 and a synchronization perturbation is written as follow.

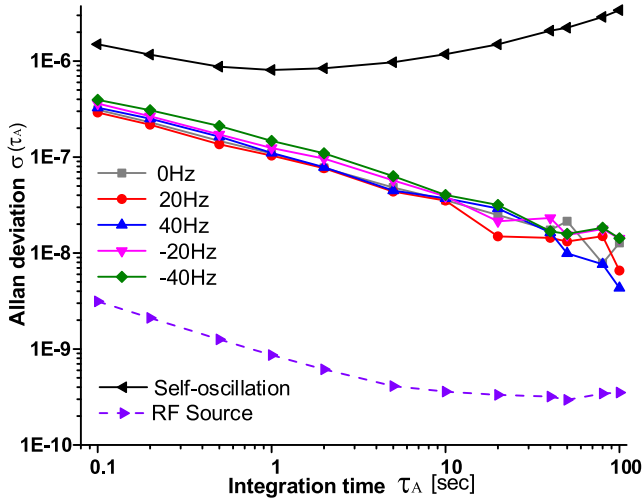

FIG. 4. Allan deviation σ of the piezoresistive oscillator at different perturbation frequency detunings $\delta\Omega$ (colored lines) and at unsynchronized state (dark line), and of the perturbation signal generated by RF source (dashed purple line).

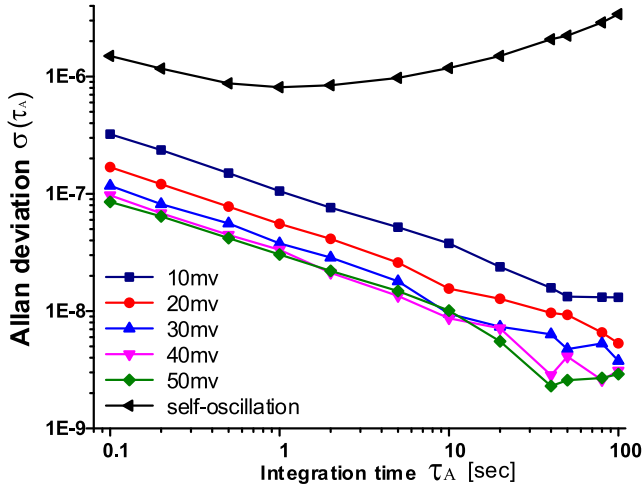

FIG. 5. Allan deviation σ of the piezoresistive oscillator at free running and at different external perturbation intensities.

$$\ddot{x} + Q^{-1}\dot{x} + x + \beta x^3 = f_0 \mathrm{sgn}(\cos\phi_t) + f_s \cos\Omega_s' \tau + \xi_1(t) + \xi_2(t)x \tag{8}$$

Using the averaging method,[13] the power spectral density of the random phase fluctuation can be derived as follow.

$$S_\phi(\omega) = \frac{4D}{4\pi^2\omega^2 + \Omega_c^2 - \delta\Omega^2} \tag{9}$$

Where ω is the modulation frequency, Ω_c is obtained in deterministic situation and D is the non-dimensional noise intensity ($D = D_d/2\pi f_0$). Noted that D_d is defined by the auto-correlation function $\xi(t)\xi(t+\Delta t) = 2D_d\delta(\Delta t)$. Allan variance is a function of the power spectral density[15] and is given as follow.

$$\sigma_A^2(\tau_A) = 2\left(\frac{2}{\Omega_0'\tau_A}\right)^2 \int_0^\infty S_\phi(\omega) \sin^4\left(\frac{\omega\tau_A}{2}\right) d\omega \tag{10}$$

Where, τ_A is the time interval, and Ω_0 is the angular frequency of free-running oscillator. The synchronization bandwidth Ω_c and the frequency detuning $\delta\Omega$ discussed here are all positive real. Assuming

$\Omega_c > \delta\Omega$, i.e. the oscillator operates in the synchronized state, and Allan deviation can be obtained

$$\sigma_A(\tau_A) = \sqrt{\frac{2\pi D}{\Omega_0'^2 \tau_A^2} \frac{(e^{-\Delta\Omega\tau_A} - 2)^2 - 1}{\Delta\Omega}} \tag{11}$$

Where $\Delta\Omega = \sqrt{\Omega_c^2 - \delta\Omega^2}$. According to Eq. 7 and Eq. 11, it is clear that the Allan deviation is a function of the synchronizing perturbation intensity (or SPR) and the frequency detuning. The dimensional noise intensity $D_d \approx 9.93 \times 10^{-4}$ is proportional to the noise spectra density which can be obtained from the spectrum analyzer. The calculated Allan deviation σ_A of the piezoresistive oscillator of different frequency detunings and perturbation intensities are shown in Fig. 6a and Fig. 6b. It should be noted that the additive noise and multiplicative noise are used to give a general description of the noise in the whole closed loop system rather than specific sources, and the data from spectrum analyzer already takes the noise from the electrical devices into account. From the experiments results and analytical results given above, we can find that a high-precision perturbation brings a good performance of frequency stability of this synchronized micromechanical oscillator. Besides, the perturbation is assumed to be a pure source in our model which might account for the one order of magnitude difference between the experimental and analytical results in Fig. 4, Fig. 5 and Fig. 6. Nevertheless, the trends that the frequency stability of the synchronized oscillator stays relatively stable in the synchronization region and can be further improved by a larger perturbation intensity agree well with the trends of the experimental data in Fig. 4 and Fig. 5.

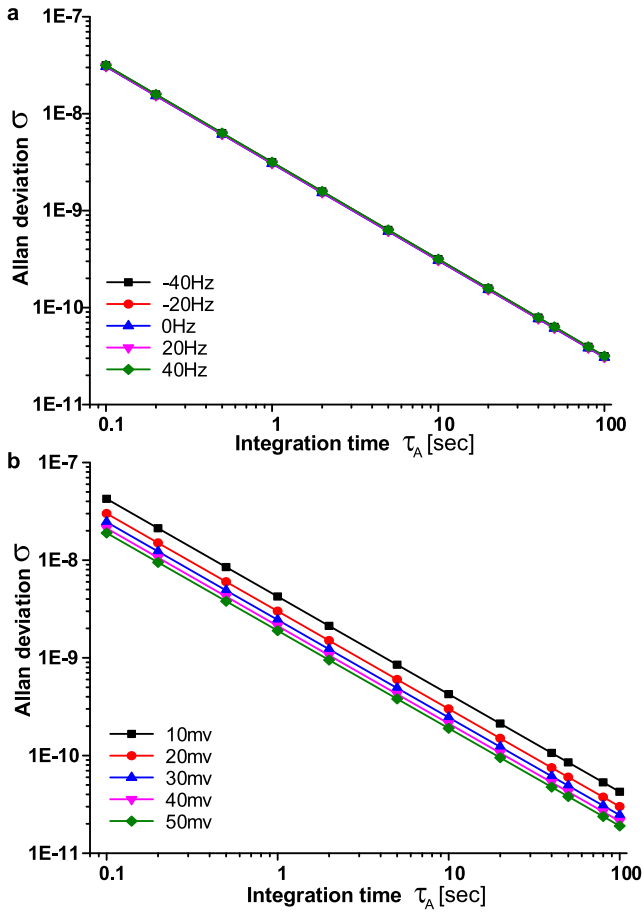

FIG. 6. Predicted Allan deviation σ of the piezoresistive oscillator (a) at frequency detunings $\delta\Omega$ varying from -40Hz to 40Hz and (b) at different external perturbation intensities varying from 10mV to 50mV.

To conclude, a piezoresistive oscillator is built up on a C-C micromechanical beam resonator and the improvement of its frequency stability is experimentally demonstrated via synchronization phenomenon. The effects of external perturbation detuning and intensity are studied experimentally and a theoretical model is built up to analyze the noise polluted oscillator and the explicit analytical formula of Allan deviation successfully explains experimental observations. The parameters such as nonlinearities (mechanical hardening and electrostatic softening), quality factor, signal to perturbation ratio and noise intensity are all influencing the final frequency stability of the oscillator. In this work, the frequency Ω_0 of our piezoresistive oscillator equals to that of the external force Ω_s once they are synchronized and their frequency ratio η is 1. However, one should be noted that sub-harmonic (e.g. $\eta = 3$) or super-harmonic (e.g. $\eta = \frac{1}{3}$) synchronization phenomena can be observed as well in micro/nanomechanical oscillator.[16]

ACKNOWLEDGMENTS

This work is financially supported by the National Natural Science Foundation of China (51575439, 51421004, 11372271 and 11432012), Natural Science Foundation of Shaanxi Province (2014jm2-5054) and 111 project (B12016). We also appreciate the support from the Collaborative Innovation Center of High-End Manufacturing Equipment and the International Joint Laboratory for Micro/Nano Manufacturing and Measurement Technologies.

[1] D. Antonio, D. H. Zanette, and D. López, Nature Communications **3**, 806 (2012).
[2] K. L. Ekinci and M. L. Roukes, Review of Scientific Instruments **76**, 61101 (2005).
[3] M. Agarwal, H. Mehta, R. N. Candler, S. A. Chandorkar, B. Kim, M. A. Hopcroft, R. Melamud, G. Bahl, G. Yama, T. W. Kenny, and B. Murmann, Journal of Applied Physics **102** (2007).
[4] B. Yurke, D. S. Greywall, A. N. Pargellis, and P. A. Busch, Phys. Rev. A **51**, 4211 (1995).
[5] D. Antonio, D. A. Czaplewski, J. R. Guest, D. Lopez, S. I. Arroyo, and D. H. Zanette, Phys Rev Lett **114**, 34103 (2015).
[6] C.-M. Lin, T.-T. Yen, V. V. Felmetsger, M. A. Hopcroft, J. H. Kuypers, and A. P. Pisano, Appl. Phys. Lett. **97**, 83501 (2010).
[7] T. Kouh, O. Basarir, and K. L. Ekinci, Applied Physics Letters **87**, 113112 (2005).
[8] M. Defoort, P. Taheri-Tehrani, and D. A. Horsley, Applied Physics Letters **109** (2016).
[9] M. Sansa, E. Sage, E. C. Bullard, M. Gély, T. Alava, E. Colinet, A. K. Naik, L. G. Villanueva, L. Duraffourg, M. L. Roukes *et al.*, Nature Nanotechnology **11**, 552 (2016).
[10] A. Pikovsky, M. Rosenblum, and J. Kurths, *Cambridge Nonlinear Science Series 12* (2003), p. 432.
[11] D. K. Agrawal, J. Woodhouse, and A. A. Seshia, Phys Rev Lett **111**, 84101 (2013).
[12] M. H. Matheny, M. Grau, L. G. Villanueva, R. B. Karabalin, M. C. Cross, and M. L. Roukes, Phys Rev Lett **112**, 14101 (2014).
[13] O. Shoshani, D. Heywood, Y. Yang, T. W. Kenny, and S. W. Shaw, Journal of Microelectromechanical Systems **25**, 870 (2016).
[14] X. Wei and A. A. Seshia, Micro & Nano Letters **8**, 107 (2013).
[15] W. F. Egan, *Frequency Synthesis by Phase Lock* (Wiley, New York, 2000).
[16] S.-B. Shim, M. Imboden, and P. Mohanty, Science (New York, N.Y.) **316**, 95 (2007).